

# Cosmological String Gas on Orbifolds

Richard Easther<sup>\*1</sup>, Brian R. Greene<sup>\*§2</sup>, Mark G. Jackson<sup>†3</sup>

*\*Institute for Strings, Cosmology and Astroparticle Physics*

*§Department of Mathematics*

*†Department of Physics*

*Columbia University*

*New York City, NY 10027*

## Abstract

It has long been known that strings wound around incontractible cycles can play a vital role in cosmology. In particular, in a spacetime with toroidal spatial hypersurfaces, the dynamics of the winding modes may help yield three large spatial dimensions. However, toroidal compactifications are phenomenologically unrealistic. In this paper we therefore take a first step toward extending these cosmological considerations to  $D$ -dimensional toroidal orbifolds. We use numerical simulation to study the timescales over which “pseudo-wound” strings unwind on these orbifolds with trivial fundamental group. We show that pseudo-wound strings can persist for many “Hubble times” in some of these spaces, suggesting that they may affect the dynamics in the same way as genuinely wound strings. We also outline some possible extensions that include higher-dimensional wrapped branes.

---

<sup>1</sup> E-mail: easther@physics.columbia.edu

<sup>2</sup> E-mail: greene@physics.columbia.edu

<sup>3</sup> E-mail: markj@physics.columbia.edu

# 1 Introduction

A great deal of effort has been expended on studying compactifications of string theory, that is, geometrical backgrounds in which four spacetime dimensions are assumed to be large while the others are unobservably small. In order to develop a complete and viable physical model, though, we must not only describe the nature of the compactification, but also understand the dynamical processes which produced it. While a compactification can be, and usually is, imposed by hand, doing so goes against the grain of the superstring program.

We are already familiar with a number of fundamental symmetries which are broken as the universe evolves. A common and reasonable assumption that the division between large and small spatial dimensions is one of the asymmetries arising naturally during the course of cosmological evolution. For example, in the very early universe all of the dimensions may have been compact with small radius and some dynamical process may have subsequently driven significant expansion in only three of the spatial dimensions. Some time ago, Brandenberger and Vafa [1] proposed just such a mechanism for a universe in which all spatial dimensions were toroidal. Here, wound strings impede cosmological expansion if they fall out of thermal equilibrium. Since two-dimensional string worldsheets generically fail to intersect in more than four spacetime dimensions, the interactions required for thermal equilibrium are not robust in more than four spacetime dimensions, giving a qualitative explanation of why spatial regions with more than three dimensions do not expand. This is an attractive proposal, since it uses the simple and intrinsically stringy winding modes. Moreover, aspects of the model were verified [3] using a numerical algorithm originally devised by Smith and Vilenkin [4] and this line of argument was recently extended to include a spectrum of branes [5].

Unfortunately, toroidal compactifications do not lead to realistic particle physics models whereas toroidal orbifolds or Calabi-Yau compactifications of string theory (or perhaps  $G_2$  compactifications of M-theory) have a better chance of yielding the particle phenomenology we observe. Obviously, it is worth rethinking the Brandenberger-Vafa mechanism in these contexts. In this paper we take a preliminary step in this direction.

A crucial ingredient of the Brandenberger-Vafa mechanism is that tori have nontrivial cycles in every dimension, and each of these cycles is a member of a family that moves throughout the torus. This is not true of more general compactifications. In particular, many toroidal orbifolds and Calabi-Yau spaces have trivial fundamental groups and thus no notion of wound strings. Without incontractible 1-cycles it would seem that one cannot expect an analog of the Brandenberger-Vafa mechanism to hold in these spacetimes. However, these spaces still support “pseudo-wound” strings – contractible strings that wrap the full spatial extent in a given direction. If these strings contract in time scales that are less than the cosmological Hubble time, they will be cosmologically irrelevant

and cannot support a modified version of the Brandenberger-Vafa scenario. However, if their contraction time scale is significantly longer than the Hubble time this raises the possibility that pseudo-wound modes can play the same role as their stable, truly wound cousins.

As an illustrative example, consider a compactification involving an elliptically fibered  $K_3$  manifold.  $K_3$  has a trivial fundamental group and yet in the neighborhood of a non-degenerate fiber the space looks locally like  $U \times T^2$  with  $U$  an open set in  $CP^1$ . A string that winds around a cycle of the  $T^2$  is not topologically stable, but in order to decay it must move over the base to one of 24 singular fibers on which it can shrink. If the  $CP^1$  base is large or asymmetric in shape (e.g. the cigar shape discussed in [6]), it is conceivable that the growth of the toroidal fibers might be inhibited by the pseudo-wound string modes over cosmologically interesting timescales.

Similarly, even though toroidal orbifolds generally have trivial fundamental groups, string configurations that would be topologically wound on the covering space must find their way to a fixed point of the group action in order to unwind. This process introduces a time scale and here we study the lifetime of such pseudo-wound strings on orbifolds. We employ the same numerical techniques used in toroidal spacetimes [3, 4] but adapt them for use on orbifolds. The  $\mathbb{Z}_4$  symmetry of the basic 2D lattice used in [4] allows us to construct several orbifolds which respect the usual supersymmetry conditions [7], and we consider:

$$T^4/\mathbb{Z}_2, T^4/\mathbb{Z}_4, T^6/\mathbb{Z}_2, T^6/\mathbb{Z}_4, T^6/\mathbb{Z}'_4, T^6/(\mathbb{Z}_2 \times \mathbb{Z}_2)$$

where  $\mathbb{Z}'_4$  acts differently than  $\mathbb{Z}_4$ , as explained below. For purposes of comparison, we also consider the “factored,” non-supersymmetric orbifolds

$$T^2/\mathbb{Z}_2, (T^2/\mathbb{Z}_2)^2, (T^2/\mathbb{Z}_2)^3, T^2/\mathbb{Z}_4, (T^2/\mathbb{Z}_4)^2, (T^2/\mathbb{Z}_4)^3.$$

In this way we study the dimensional and topological dependence of various scenarios.

Our numerical simulations assume that the background spacetime is not evolving, so while our results shed light on the stability and persistence of string networks on toroidal orbifolds, they do not directly describe the dynamical evolution of these spaces. Moreover, the Brandenberger-Vafa scenario requires that the dilaton is evolving freely [2], so the spacetime dynamics cannot be governed by general relativity. If the dilaton is fixed, the low energy limit of string theory reduces to general relativity and string networks actually enhance the expansion rate since they have negative pressure. However, as shown in Appendix A of Ref. [2], string networks do not induce rapid expansion in dilaton gravity, and the subspaces where the strings do not annihilate will expand more slowly than those in which they do. The mechanism that fixes the dilaton is not well understood, but it is reasonable to assume that it is related to the physics which clamps the values of the moduli that set the size of the internal space, which must happen if the compactification is to be stable. This leads to a consistent picture: in addition to

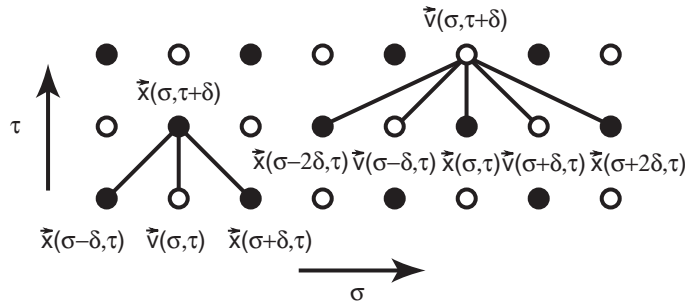


Figure 1: Positions and velocities of the string are evolved based on nearby positions and velocities from the previous timestep.

a running dilaton, the Brandenberger-Vafa scenario requires that the moduli be free to evolve if it is to induce the anisotropy between the three large directions we observe and the remaining compact directions, and both the moduli and dilaton are fixed after the Brandenberger-Vafa mechanism has had time to work.

In Section 2 we review the numerical techniques used in the simulation, including the representation of the orbifolds we study. In Section 3 we present the results of the simulations and discuss their significance. In Section 4 we go on to discuss some general features of string and brane gas models in the context of Calabi-Yau compactifications, and we identify possible extensions to this work.

## 2 Numerical simulation

### 2.1 The Smith-Vilenkin Lattice

Our simulations use the lattice model constructed by Smith and Vilenkin [4]. The worldsheet gauge is chosen, so we must satisfy the conditions

$$\mathbf{X}' \cdot \dot{\mathbf{X}} = 0, \quad (2.1)$$

$$\mathbf{X}'^2 + \dot{\mathbf{X}}^2 = 1, \quad (2.2)$$

as well as the equation of motion

$$\ddot{\mathbf{X}} - \mathbf{X}'' = 0, \quad (2.3)$$

where primes and overdots denote derivatives with respect to the worldsheet coordinates  $\sigma$  and  $\tau$ .

By discretizing the worldsheet coordinates as in Figure 1, Eq. (2.1) and Eq. (2.2) become

$$\mathbf{u}' \cdot \dot{\mathbf{v}} = 0, \quad (2.4)$$

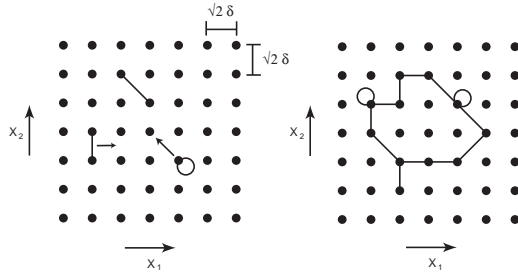


Figure 2: (Left) Links in the string are constructed from three types of segments, moving at a velocity such that the combined energy (due to velocity and tension) in each is uniform. (Right) A typical string.

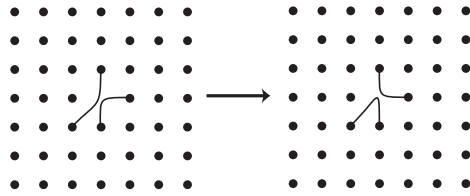


Figure 3: Interactions are performed via intercommutation at a single point, which has been removed for clarity.

$$\mathbf{u}'^2 + \dot{\mathbf{v}}^2 = 1 \quad (2.5)$$

where we have defined

$$\mathbf{u}(\sigma, \tau) \equiv [\mathbf{X}(\sigma + \delta, \tau) - \mathbf{X}(\sigma - \delta, \tau)]/2\delta, \quad (2.6)$$

$$\mathbf{v}(\sigma, \tau) \equiv \{[\mathbf{X}(\sigma, \tau + \delta) - \frac{1}{2}[\mathbf{X}(\sigma + \delta, \tau) + \mathbf{X}(\sigma - \delta, \tau)]]\}/\delta. \quad (2.7)$$

The solutions to these equations are

$$\mathbf{X}(\sigma, \tau + \delta) = \frac{1}{2}[\mathbf{X}(\sigma + \delta, \tau) + \mathbf{X}(\sigma - \delta, \tau)] + \mathbf{v}(\sigma, \tau)\delta, \quad (2.8)$$

$$\begin{aligned} \mathbf{v}(\sigma, \tau + \delta) &= \frac{1}{2}[\mathbf{v}(\sigma + \delta, \tau) + \mathbf{v}(\sigma - \delta, \tau)] \\ &+ [\mathbf{X}(\sigma + 2\delta, \tau) - 2\mathbf{X}(\sigma, \tau) + \mathbf{X}(\sigma - 2\delta, \tau)]/4\delta. \end{aligned} \quad (2.9)$$

These are gauge preserving and become exact solutions to the differential equations Eq. (2.1) and Eq. (2.2) as  $\delta \rightarrow 0$ .

It is essential that the initial conditions respect the gauge. This is ensured by also discretizing the target space and allowing only three types of links, as shown in Figure 2 (our target space grid has been rotated from that of [4]). The first type has  $|\mathbf{u}| = 1$  and  $\mathbf{v} = 0$ . Its end points are separated by  $|\Delta\mathbf{X}| = 2\delta$ , which implies that two components of

$\Delta\mathbf{X}$  are  $\pm\sqrt{2}\delta$  and the others are zero. Such links are “fully stretched” and are at rest. The second type has  $|\mathbf{u}| = |\mathbf{v}| = 1/\sqrt{2}$ , implying that one component of  $\Delta\mathbf{X}$  is  $\pm\sqrt{2}\delta$  and the others are zero, and one component of  $\mathbf{v}$  is  $\pm\frac{1}{\sqrt{2}}$  and the others are zero. Such partially contracted links move at 0.707 light speed perpendicular to themselves. The third type has  $\mathbf{u} = 0$  and  $|\mathbf{v}| = 1$ . Its end points are degenerate, with  $\Delta\mathbf{X} = 0$ . Two components of  $\mathbf{v}$  are  $\pm\frac{1}{\sqrt{2}}$  and the others are zero. Such links are fully contracted and move at light speed diagonal to the coordinate axes. A 2D lattice is shown here but the generalization to higher dimensions is obvious.

String interactions are achieved via the intercommutation of two strings which pass through the same lattice site in the target space, as shown in Figure 3. This preserves the gauge constraint exactly, as well as energy, momentum and angular momentum. We specify the coupling constant by assigning a probability  $P$  that strings in such a configuration will in fact intercommute.

## 2.2 Simulation of strings on orbifolds

In Figure 4 we show how  $G = \mathbb{Z}_2$  acts on the manifold  $M = T^2$  to produce the pillow-shaped orbifold  $\Gamma = T^2/\mathbb{Z}_2$  with fixed points  $O, P, Q,$  and  $R$ . Construction of  $T^2/\mathbb{Z}_4$  is similar, producing a space with three fixed points. Higher-dimensional orbifolds are of course more difficult to visualize, but are mathematically straightforward. We construct  $\Gamma = T^4/\mathbb{Z}_2, T^4/\mathbb{Z}_4, T^6/\mathbb{Z}_2,$  and  $T^6/\mathbb{Z}_4$  by letting  $z_i, i = 1, \dots, D/2,$  be the variables on a complex torus defined by  $z_i \cong z_i + 1 \cong z_i + i$ . The group acts on these as follows:

$$(z_1, z_2) \mapsto (e^{i\theta} z_1, e^{-i\theta} z_2)$$

with  $\theta = \pi$  for  $G = \mathbb{Z}_2$  and  $\theta = \pi/2$  for  $G = \mathbb{Z}_4$ . For  $D = 6,$   $z_3$  is left invariant under the group action. We construct  $T^6/\mathbb{Z}_4$  by acting as

$$(z_1, z_2, z_3) \mapsto (e^{i\pi/2} z_1, e^{i\pi/2} z_2, e^{i\pi} z_3)$$

and finally  $T^6/(\mathbb{Z}_2 \times \mathbb{Z}_2)$  by

$$\begin{aligned} (z_1, z_2, z_3) &\mapsto (e^{i\pi} z_1, e^{i\pi} z_2, z_3) \\ (z_1, z_2, z_3) &\mapsto (z_1, e^{i\pi} z_2, e^{i\pi} z_3). \end{aligned}$$

We refer to these as the “supersymmetric orbifolds”. For the “factored” cases  $(T^2/\mathbb{Z}_2)^{D/2}$  and  $(T^2/\mathbb{Z}_4)^{D/2}$  each  $z_i$  is acted on by a separate copy of  $G$ .

We simulate string evolution on these spaces as follows. When identifying interactions, the group acts on the position of each string link, producing an orbit. Identical orbits (rather than identical positions) then give rise to intercommutation, with the group action information included in the string’s link for future string evolution.

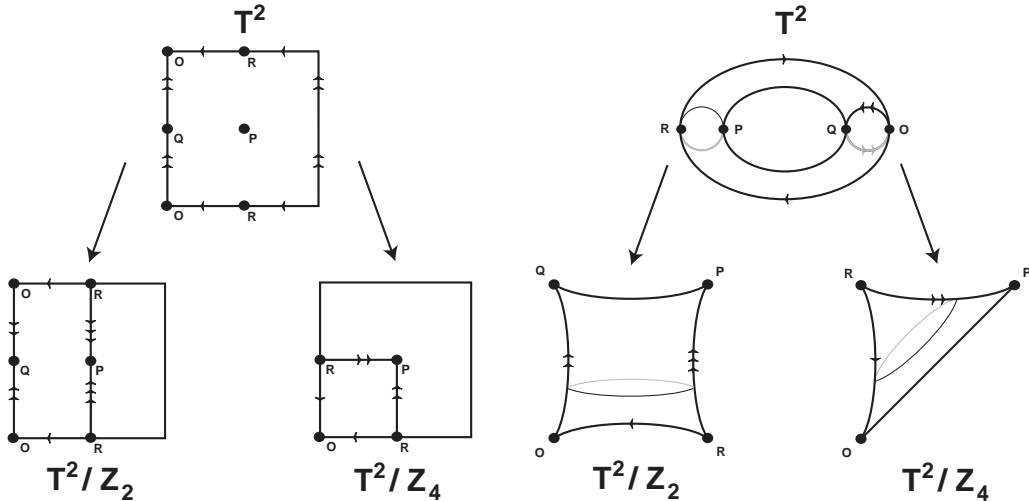


Figure 4: Orbifolding takes a smooth geometry and creates singularities if the group action has fixed points. In these examples, we take  $T^2 \rightarrow T^2/\mathbb{Z}_2$  and  $T^2 \rightarrow T^2/\mathbb{Z}_4$ .

### 3 Simulations and Results

We begin by checking our simulation algorithm against previous codes, and then perform two sets of computations. In the first we keep the intercommutation probability at  $P = 1$ , and vary the topology. In the second, we focus on topologies which had potential for thermalization in more than 3+1 dimensions, and study the impact of varying  $P$ .

#### 3.1 Critical density computation

Previous studies have calculated the critical density in string thermodynamics, or the maximum allowed short string density [3, 4, 8]. We first determine this density as a computational check. We define a “long” string in the same way as previous analyses: a string is “long” if its extent in at least one dimension is approximately the length of that dimension. Using a string network consisting of 100,000 string links and units such that energy is measured in links and length in  $\delta$ , we obtain the following critical densities:

$$\begin{aligned}
 D = 3 : & \quad 0.1715 \pm 0.0083 \\
 D = 4 : & \quad 0.0560 \pm 0.0009 \\
 D = 5 : & \quad 0.0269 \pm 0.0003
 \end{aligned}$$

These agree to within a few percent of the results found in the literature [3, 4, 8]. While the difference exceeds the uncertainty in the fit, the results also depend weakly on the overall lattice size, or the specific details of the interaction code when more than two

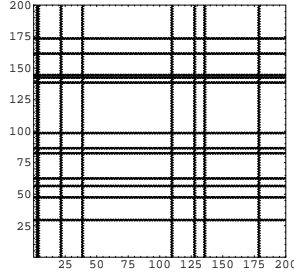


Figure 5: Typical initial winding configurations for  $T^2$ . For clarity we have only drawn 20 initially wound strings; in the simulations there were between 50 and 100.

strings intersect at a point, and these systematic effects are most likely the origin of the discrepancy.

### 3.2 Unwinding rate at constant coupling

Our first investigation compares the rates of string unwinding in different topologies in the “strong coupling” regime of  $P = 1$ . This allows the most efficient interactions, and hence the greatest possible change to some initially wound state. We chose the dimensions so that each space has volume of  $\sim (200\sqrt{2}\delta)^D$ , and a total of 40,000 wound string links. For example, on  $T^2$  we choose  $L = 200\sqrt{2}\delta$  and 100 wound strings, whereas on  $T^6/\mathbb{Z}_4$  we choose  $L = 252\sqrt{2}\delta$  and 80 wound strings. As shown in Figure 5, the strings are initially wrapped at random around the dimensions, with half of the string links being fully extended in a zig-zag pattern and half the links being fully kinetic with velocity directions chosen at random. This allows us to construct initial configurations with random velocities, so that the strings have a fair chance of moving around and interacting. This kind of winding configuration was one of several proposed in [3], and suited our purposes best. The string density was kept low so that complications arising from the Hagedorn transition (see [8, 9, 10]) were avoided and there was no obstacle to all strings becoming small.

To determine if the result was density-dependent, we then performed simulations where the lattice length was reduced by factors of 3 and 7, keeping the number of wound strings the same (note that the number of links in a wound string is proportional to the length of the dimension). This significantly increases the density: when the 6D lengths are reduced by a factor of 3, the density changes by a factor of  $3^5 = 243$ .

The simulations were run for 20 Hubble times<sup>4</sup>, which in the lowest density simulation,

---

<sup>4</sup>We use the term ‘Hubble time’ to denote the time required for light to propagate across the size of the universe. This usage is slightly loose since we are not working with an expanding background.



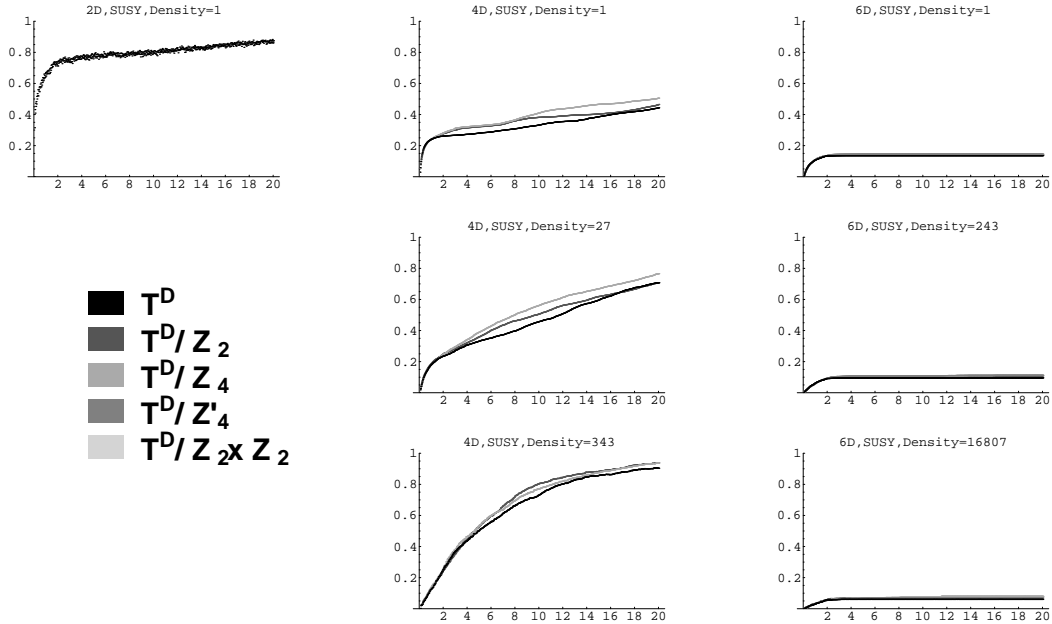


Figure 6: Plots of  $\rho_{small}/\rho_{total}$  on supersymmetric orbifolds as a function of Hubble time for different dimensionalities and densities. The 2D cases were only done at the lowest density since we quickly ran into Hagedorn issues.

was 4000 time steps. In Figure 6 we plot the ratio of small string energy density  $\rho_{small}$  to the total energy density  $\rho_{total}$  for each configuration. Since all strings began large, this ratio measures the efficiency with which the strings interact to form small strings and the speed with which this happens determines whether the “pseudo-wound” strings can have an impact on the overall cosmological evolution. For these simulations, we could not use the “extent” criteria of Refs [3, 4, 8], as orbifolds do not allow simple definitions of length in each dimension. Instead, our criterion for a string to be “long” is that the total string length is at least  $L/2$ . This is not as descriptive as measuring the string’s extent in each dimension, but since thermodynamics creates a large gap between “small” and “large” strings we believe this serves our purpose [3, 8].

Our initial configuration, with half of the links purely kinetic, allows half of the string to be “slack”. Thus it can lose up to half of its links and still be wound around the torus or wrap around the largest cycle of the orbifold. Since we expect that strings can shed this slack quickly, the real indication of unwinding is how quickly the short string density rises after reaching  $\rho_{small}/\rho_{total} \approx 0.5$ .

The toroidal cases behaved as expected, in agreement with Ref. [3]. With  $D = 2$  the long strings immediately fragmented to small strings, whereas with  $D = 4$  and  $D = 6$  the long strings persisted, as expected from naive phase-space arguments based on the dimensionality of strings.

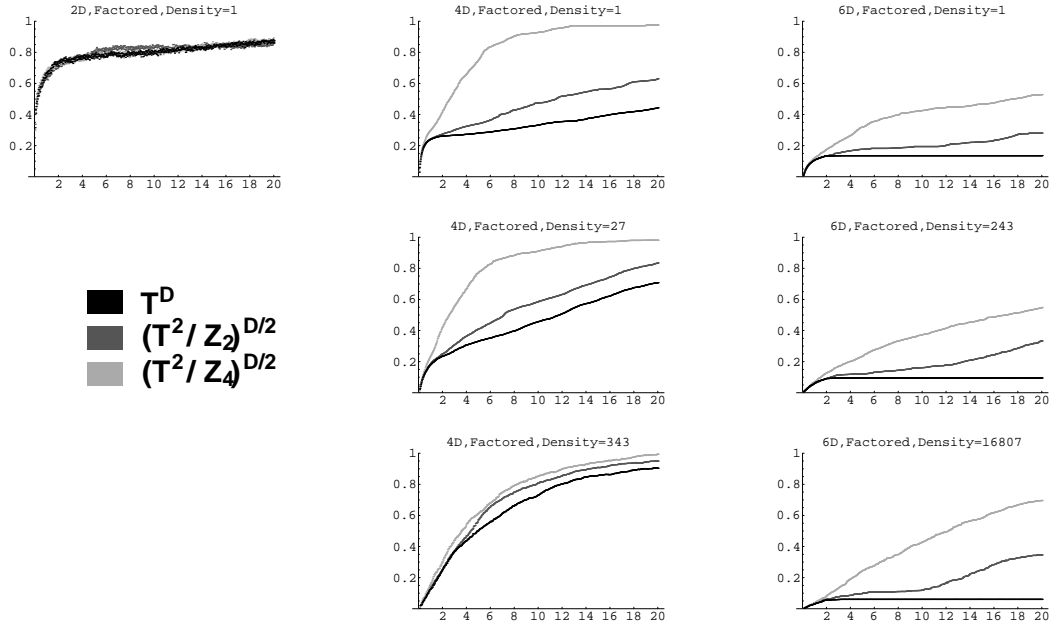


Figure 7: Plots of  $\rho_{small}/\rho_{total}$  on factored, non-supersymmetric orbifolds as a function of Hubble times for different dimensionalities and densities. The 2D cases were only done at the lowest density since we quickly ran into Hagedorn issues.

The results for the orbifold simulations are similar. In all supersymmetric cases we studied, the unwinding rate was nearly identical to the toroidal case. This apparent indifference to topology is presumably due to the high codimension of the fixed point sets, which makes it difficult for the pseudo-wound strings to find a path that results in their unwinding. In both of the 4 and 6 dimensional orbifolds we study, the singularities are codimension 4, providing a significant phase space to support long pseudo-wound strings.

To test this idea, we simulated examples where the topology can be factored into products of 2-dimensional orbifolds:  $(T^2/\mathbb{Z}_2)^{D/2}$  and  $(T^2/\mathbb{Z}_4)^{D/2}$ , yielding lower codimension fixed point sets. As explained previously, these were constructed analogously to the supersymmetric orbifolds, except that each complex torus now has its own group action. In these examples the string can unwind within the individual 2D orbifolds around which it was initially wound. Intuitively, we expect these models to produce different results from the analogous toroidal cases, except for  $D = 2$  where the strings will overlap regardless of topology. We emphasize that these spaces are not realistic candidates for compactification.

The  $T^2/\mathbb{Z}_2$  case is very similar to the torus, immediately achieving  $\rho_{small}/\rho_{total} \approx 0.5$  and thus unwinding quickly. For other  $(T^2/\mathbb{Z}_2)^{D/2}$  spaces, the unwinding is more efficient than for the torus, but the overall dynamics do not differ significantly. The  $(T^2/\mathbb{Z}_4)^{D/2}$

cases do differ, however. For  $D = 2$ , the story is identical to  $T^2$ . In  $D = 4$ , however, the behavior is nearly identical to that of  $T^4$  for only about 1 Hubble time. After this, the strings continue to contract, taking only  $\sim 3$  Hubble times to achieve  $\rho_{small}/\rho_{total} \approx 0.5$  and eventually producing completely short strings. In a cosmological setting, this rapid unwinding would not be compatible with the Brandenberger-Vafa scheme. The larger configuration space associated with the  $(T^2/\mathbb{Z}_4)^3$  prevents rapid string unwinding, although string contraction is more efficient than that on  $T^6$  (see Figure 7).

The intuitive picture of the decay of long strings as a function of dimensionality is built around two extremes. A low dimensionality has high string density and thus allows quick but not necessarily complete fragmentation, due to the Hagedorn transition favoring the creation of long (and thus likely wound) strings. A high dimensionality has slow (if any) fragmentation, though once fragmentation takes place there is no obstacle to all strings remaining small. How the system behaves in between these extremes depends on the topology. The 2-dimensional simulations were nearly identical (immediate, but not complete, unwinding) as were the 6-dimensional cases (slow or nonexistent unwinding). All 4-dimensional cases begin with moderate unwinding. After approximately one Hubble time the  $T^4$  and  $(T^2/\mathbb{Z}_2)^2$  fragment very slowly, whereas  $(T^2/\mathbb{Z}_4)^2$  continues to fragment moderately until all strings are small. This is because during the first Hubble time fragmentation is only possible due to mutual interaction. After this, once a string has had enough time to contract around a fixed point due to its tension, it can self-interact. This difference is explained by the topology:  $T^2/\mathbb{Z}_4$  demands that strings wound in the covering space self-intersect, whereas the others do not.

### 3.3 Varied probability of intercommutation

Of the topologies examined,  $(T^2/\mathbb{Z}_4)^{D/2}$  has the greatest potential for string unwinding, possibly allowing thermalization in more than  $3 + 1$  dimensions. Even though this space is not a realistic candidate for compactification, it allows us to perform one other useful test. The previous calculations were performed at an intercommutation probability of 1, but perhaps for sufficiently low interaction rates the strings would not interact enough to unwind. To explore this, we repeated the simulation on  $(T^2/\mathbb{Z}_4)^2$  for up to 5 Hubble times with  $0 \leq P \leq 1$ , effectively varying the value of the string dilaton, which determines the intercommutation probability. As shown in Figure 8, for small coupling the unwinding rate sharply rises with  $P$  until  $P \sim 0.4$ , beyond which it stabilizes.

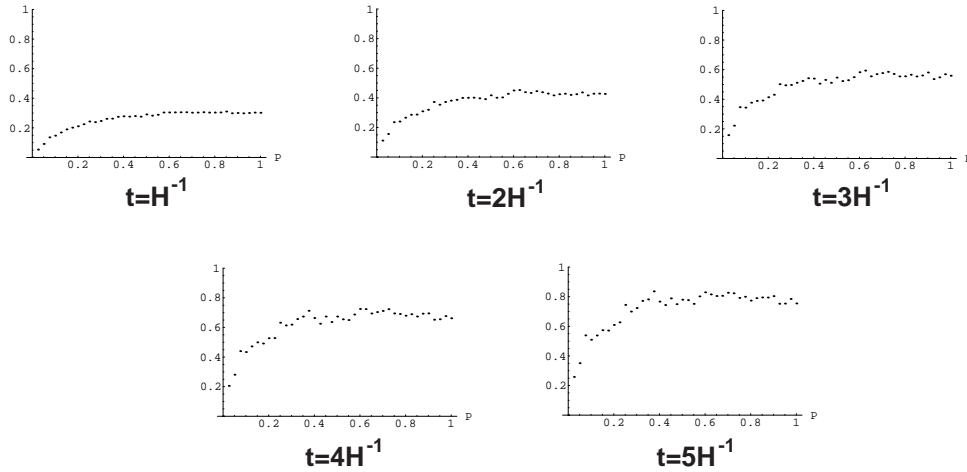


Figure 8: Plots of  $\rho_{small}/\rho_{total}$  on  $(T^2/\mathbb{Z}_4)^2$  with variable intercommutation probabilities  $P$  at different time scales.

## 4 Branes and General Compactifications

Our simulations show that pseudo-wound strings on supersymmetry preserving orbifold compactifications have long lifetimes. Consequently, they may play an important cosmological role by inducing anisotropic cosmological expansion similar to that seen with toroidal compactifications. So far we have focused solely on strings, but brane wrappings of higher dimensional cycles can be important cosmologically, as emphasized in Ref. [11]. However, Ref. [11] restricts its analysis to toroidal spaces and it is worth briefly considering such ideas in more general compactifications.

In Refs [1, 11], the authors employ the moduli space approximation, studying the cosmological evolution of the radial moduli of the assumed spatial nine-torus topology. Although this approximation has limited validity in cosmological settings, we also use it to get a qualitative understanding of the dynamics when branes are wrapped on more complex compact spaces. Imagine that we compactify nine spatial dimensions and allow the moduli of the compactification to be time dependent. For example, assume that the compactification involves the simplest non-toroidal Calabi-Yau space, namely  $K_3 \times T^5$  in type IIA string theory.<sup>5</sup> Just as in [11], the higher dimensional branes with  $p = 8, 6, 4$  generically intersect in nine space dimensions, and quickly thermalize, leaving 2-branes and 1-branes. We expect wrapped 2-branes to dominate over wrapped 1-branes in the energy-momentum tensor, so 2-branes will initially dominate the cosmology.

<sup>5</sup>Here we are specifying the asymmetric topology by hand and asking if there is a natural mechanism that yields an asymmetric geometry.

The holomorphic 2-cycles in this product space are the 2-cycles on the  $K_3$  and the 2-cycles on the  $T^5$ , since  $K_3$  has no 1-cycles to hook up with the 1-cycles on the  $T^5$ . Naive dimension counting then suggests that thermal fluctuations in the early universe cause some 5-dimensional submanifold to grow large and that efficient 2-brane/anti-2-brane annihilations in this submanifold allow the geometrical asymmetry to grow. A natural scenario, independently suggested in [12], is that the  $T^5$  fluctuates to a large size, leaving the  $K_3$  small, and continues to grow ever larger while the 2-branes wrapping the 2-cycles in the  $K_3$  keep it small. However, this scenario is not unique. Return to the example in the Introduction, and imagine that the  $K_3$  is elliptically fibered over a  $CP^1$  base and that the initial thermal fluctuation involves  $CP^1 \times T^3$ . Wrapped 2-branes efficiently annihilate in this subspace allowing it to continue to grow while 2-branes and 1-branes wrapping the smaller dimensions do not efficiently annihilate and hence impede their growth. Within the 5-manifold  $CP^1 \times T^3$  we then expect a thermal fluctuation to drive a larger 3-dimensional subspace within which wrapped strings can efficiently annihilate. Since  $CP^1$  has no 1-cycles, the preferred choice would be a large  $CP^1 \times S^1$  so that wrapped strings keep the remaining  $T^2$  small. But if the  $T^3$  should fluctuate large first, it is hard to see what would subsequently stabilize the  $CP^1$  at small size.

If, instead, we chose the initial topology to be a Calabi-Yau three-fold  $M$  times, say, a  $T^3$ , how would things change? At first sight, one might imagine that the story is essentially the same. Some 5-dimensional manifold is driven large by a thermal fluctuation, and within this space a 3-dimensional subspace grows larger still, while wound 2-branes and 1-branes keep all other dimensions small. However, the nontrivial holomorphic cycles in a generic Calabi-Yau space  $M$  are isolated. This means that the annihilation of the branes wrapping these cycles is enormously more efficient than in the toroidal cases. For example, if a thermal fluctuation should drive  $M$  to grow momentarily larger than the  $T^3$ , dimension counting shows that 2-brane annihilation in 6-dimensional space is not efficient and thus leads us to believe that further expansion would be impeded. However, if the cycles are isolated, the branes and anti-branes which we assume to be evenly distributed with no net winding number, immediately annihilate, allowing the space to continue growing.

A potential way out of this conclusion is to note that although the holomorphic homology generators are generically isolated, sufficiently high multiples can be part of continuous families that sweep through the Calabi-Yau manifold. If branes can wrap these cycles as independent states, their annihilation would once again be inefficient, constricting expansion. Even so, a variety of geometrical evolutions might follow. For example, imagine that  $M$  is  $K_3$  fibered and that the  $K_3$  fibers are themselves elliptically fibered (over a twisted product of two copies of  $CP^1$ ). Various combinations of, say, the  $CP^1$ s in the base and the  $T^3$  or its submanifolds could receive the thermal fluctuation driving a large 5-dimensional submanifold while wrapped branes keep all other dimensions small. For instance, if  $CP^1 \times T^3$  gets large we are in the same situation as in the last paragraph.

In some of the above toy scenarios, the geometrical route we illustrated involved including part of the Calabi-Yau space or the  $K_3$  into the large spacetime manifold, partially erasing the motivation for the initial choice of vacuum topology. If the Calabi-Yau space is multiply connected or if, using the results of the last section, it is simply connected but has a sufficiently robust spectrum of pseudo-wound strings, then we can imagine a scenario in which the Calabi-Yau stays small. Namely, in  $M \times T^3$  if a two-dimensional subspace of  $M$  together with the  $T^3$  should initially become larger than the other dimensions and if the  $T^3$  then receives an additional thermal fluctuation to large size while wound or pseudo-wound strings keep the somewhat asymmetric Calabi-Yau space small, we would evolve into the more familiar situation of a small Calabi-Yau space for the extra dimensions. Moreover, in the moduli space approximation, some Calabi-Yau spaces simply do not have the necessary flexibility for all independent subspaces to get large (e.g. examples with one Kahler moduli) and hence we would then expect a thermal fluctuation to make either the  $T^3$  large from the outset, or the whole of  $M$  large from the outset. If wound or pseudo-wound strings can impede the growth of  $M$ , this would favor  $T^3$  getting large, returning us to the usual scenario of a small Calabi-Yau space.

## 5 Conclusion

We have studied the unwinding time scale for pseudo-wound strings on toroidal orbifolds to decay to short string states and found that in cases relevant for supersymmetric string compactifications the time scales can be many times the Hubble time. This suggests that such strings may play an important cosmological role, a prospect that is worthy of further study. Ideally, one would tackle this problem in a dynamical spacetime, fully incorporating the general relativistic backreaction of the strings on the geometry. This would then permit us to take up the question of geometrical homogeneity within the compact spatial dimensions. Additionally, while some work has been done on extending the Brandenberger-Vafa mechanism from string gases to brane gases, there is much more to be done. As we briefly mentioned, Calabi-Yau manifolds have numerous non-trivial cycles around which branes can wrap but since these cycles are often isolated, the subsequent dynamics can be quite different from what one expects on the torus and it would be interesting to determine the resulting cosmological implications. Finally, while this scenario can produce an initial anisotropy between the large and small directions, it does not guarantee that the compactification is stable at late times, and this problem needs to be addressed separately.

## Acknowledgments

We are grateful to R. Brandenberger, D. Easson and A. Vilenkin for useful discussions. The work of R.E. is supported by the Columbia University Academic Quality Fund and the Department of Energy. The work of B.R.G. is supported in part by the DOE grant DE-FG02-92ER40699B. M.G.J. is supported by a GAANN Fellowship from the United States Department of Education and by a Pfister Fellowship. ISCAP gratefully acknowledges the generous support of Ohrstrom Foundation.

## References

- [1] R. Brandenberger and C. Vafa, *Nucl. Phys.* **B316**, 391 (1989)
- [2] A. A. Tseytlin and C. Vafa, *Nucl. Phys.* **B372**, 443 (1992), hep-th/9109048.
- [3] M. Sakellariadou, *Nucl. Phys.* **B468**, 319 (1996), hep-th/9511075.
- [4] A. G. Smith and A. Vilenkin, *Phys. Rev.* **D36**, 990 (1987).
- [5] R. Brandenberger, D. A. Easson and D. Kimberly, *Nucl. Phys.* **B623**, 421 (2002), hep-th/0109165.
- [6] B. R. Greene, A. D. Shapere, C. Vafa, and S. T. Yau, *Nucl. Phys.* **B337**, 1 (1990).
- [7] L. Dixon, J. Harvey, C. Vafa and E. Witten, *Nucl. Phys.* **B261**, 678 (1985); L. Dixon, J. Harvey, C. Vafa and E. Witten, *Nucl. Phys.* **B274**, 285 (1986).
- [8] M. Sakellariadou and A. Vilenkin, *Phys. Rev.* **D37**, 885 (1988).
- [9] J. J. Atick and E. Witten, *Nucl. Phys.* **B310**, 291 (1988).
- [10] D. Mitchell and N. Turok, *Phys. Rev. Lett.* **58**, 1577 (1987); Imperial College report, 1987 (unpublished).
- [11] S. Alexander, R. Brandenberger, and D. Easson, *Phys. Rev.* **D62**, 103509 (2000), hep-th/0005212.
- [12] D. Easson, hep-th/0110225.